RSC Advances

ROYAL SOCIETY OF CHEMISTRY

www.rsc.org/advances

Journal Name

COMMUNICATION

Enhanced biological performance on nano-microstructured surfaces assembled by $SrTiO_3$ cubic nanocrystals

Received 00th January 20xx,
Accepted 00th January 20xx

DOI: 10.1039/x0xx00000x

www.rsc.org/

Guohui Shou,[a] Lingqing Dong,[a] Xiaozhao Wang,[a] Kui Cheng,[a] Wenjian Weng[a]*

Controlling protein adsorption on material surface can offer significant opportunities in terms of engineering the material-cell interactions. In this work, $SrTiO_3$ cubic nanocrystals exposed with {100} facets, which was proved to have strong protein affinity previously, were used to assemble nano-microstructured surface. We demonstrated that the nano-microstructured surface with highly stacking density of the nanocrystals had enhanced cellular responses in cellular adhesion and proliferation compared to that of the (100)-terminated $SrTiO_3$ single crystal substrate. The enhancement is attributed to more interaction sites resulting from heavy protein adsorption on {100} facets of the $SrTiO_3$ cubic nanocrystals, and more appropriate cell growth microenvironment arising from the nanocrystals stacked nano-microstruture. The two factors are suggested to play critical role in material-cell interactions. The $SrTiO_3$ cubic nanocrystals are powerful units to assemble surface nano/microstructure with highly biological responses.

In biological view, the first event occurring within few seconds is protein adsorption on the material surface.[1] The adsorbed protein acts like a bridge between cells and implant materials, and plays an important role in regulating cellular behavior.[2, 3] Hence, the surface modifications with stronger protein affinity should facilitate subsequent cellular responses.[4, 5]

Many factors for materials such as surface chemical composition, polarity and hydrophilicity influence the interaction with proteins.[6, 7] For wettability, proteins are more likely to adsorb on the hydrophobic surface.[8, 9] For surface charge, if the surface and the protein are opposite charges, there is a stronger interaction between them.[10, 11] All of these factors are believed to originate from surface atomic kinds and their arrangements. If a fixed crystalline material is adopted, its facets become a decisive factor. Titania nanotubes can initiate and template the self-assembly of enzymes protein, and this is uniquely associated with the anatase (001) surface of titania nanotubes and does not occur on other facets.[12] The adsorbed protein is affected by the underlying atomic structure of the nanocrystal surface, and it appears that proteins adsorb with a higher affinity on the Au {111} facet than on the Au {100} facet.[13] Previously, we also reported selective protein adsorption behavior of shape-controlled $SrTiO_3$ nanocrystals, proteins such as albumin and salmine, immunoglobulin and protamine attain high adsorption on the {100} facets, while no protein is found on {110} facets.[14]

In addition, nano-microstructured surfaces have been proven to result in better cellular responses because the nano-microstructures can provide more appropriate environment for cell growth and osseointegration establishment.[4, 15, 16] The osteoblasts are found to likely adhere and proliferate on the surface with nano-microstructures.[17, 18] And the topography with peaks and valleys promoted the cells to have more adhesion focal points.[19] When the density of the structural units changes on nanoscale, cells more likely migrate to denser areas rather than topographically sparser areas.[20]

When a cell adheres to a surface, the cell usually interacts with the adsorbed protein layer not directly with the material itself. Protein conformation can be changed upon adsorption, and different materials can lead to changes in protein adsorption.[21, 22] The amounts and conformations of adsorbed proteins can dictate cellular response to a biomaterial.[23, 24] In this work, nano-microstructured surfaces were assembled using $SrTiO_3$ cubic nanocrystals whose {100} facets have a strong affinity with proteins.[14] The protein conformation on the nanocrystals based surfaces is considered as the same because only $SrTiO_3$ {100} facets on the surfaces were exposed. The bovine serum albumin (BSA) adsorption and MC3T3-E1 cellular behavior on the nano-microstructured surfaces were evaluated. The influence of stacking density of the cubic nanocrystals was also discussed.

[a] *School of Materials Science and Engineering, State Key Laboratory of Silicon Materials, Zhejiang University, Hangzhou 310027, China*
** Corresponding author. Tel. and Fax : +86 571 87953787，E-mail address: wengwj@zju.edu.cn*

The $SrTiO_3$ cubic nanocrystals were obtained by a hydrothermal synthesis process. For a typical experiment, 0.26 ml of $TiCl_4$, 0.7 g of $SrCl_2$ and 4 g of LiOH were mixed with deionized water. All the processes were under ice-water bath. Then the solution was put into a dried Teflon-lined stainless steel autoclave. And the autoclave was sealed and heated at 200 °C for 48 h in an electric oven. The product as the precipitate at the boom was washed thoroughly with deionized water for three times to remove the residual contamination. And then the product was dried at 60 °C for 6 h. Spin-coating was used to prepare $SrTiO_3$ cubic nanocrystals based surfaces. The stacking density of the nanocrystals on surfaces could be changed by setting different spinning speeds with spinning time of 40 seconds. The 10×10 mm of the (100)-terminated $SrTiO_3$ single crystal was used as substrate in this work. All of them were put into Muffle furnace for heat-treatment at 500 °C for 60 min in order to make nanocrystals stably adhere on the substrate.

The phase of $SrTiO_3$ nanocrystals was measured by X-ray diffraction (XRD) analysis (PANalytical, X'Pert PRO, Cu-Kα). Surface chemical composition of the $SrTiO_3$ nanocrystal was characterized by an X-ray photoelectron spectroscopy (XPS, Kratos AXIS Ultra DLD). The microstructures of the $SrTiO_3$ nanocrystals and the resulting surfaces were characterized by a field emission scanning electron microscopy (FE-SEM, Hitachi, SU-70) and transmission electron microscopy (TEM, Philips Tecnai F20).

In order to study the ability of protein adsorption of the nano-microstructured surfaces, bovine serum albumin (BSA, 99%, Sigma–Aldrich) was used, and dissolved in phosphate buffer solution (PBS) at pH 7.4 to form a solution with a concentration of 1 mg/ml. The nano-microstructured surfaces were soaked in the solution for 24 hours to adsorb the protein. The amount of protein adsorption was measured by the optical density (OD) of supernatant liquid at 450 nm with a microplate reader (Multiskan MK3). And then the OD value was converted to concentration using the standard curve line.

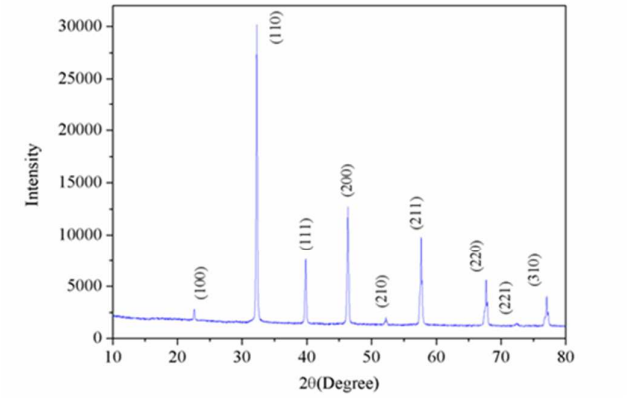

Figure 1. XRD pattern of the $SrTiO_3$ nanocrystals.

Mouse pre-osteoblastic MC3T3-E1 cells (CRL-2594, ATCC) were cultured in alpha minimum essential media (Gibco) and incubated under standard cell culture conditions at 37 °C in an atmosphere of 5% CO_2. Cell adhesion and proliferation were measured by cell counting kit-8 (CCK-8) assay. Briefly, cell cultured at a density of 5×10^4 cells /cm^2 were seeded on $SrTiO_3$ cubic nanocrystals films into a 24-multiwell plate. CCK-8 was added in the wells as the concentration ratio of 1:10 with culture solution. After that, the optical density (OD) of supernatant liquid was measured at 450 nm with a microplate reader after cultured. Cells after 1 day and 3 days incubation were fluorescently labeled by Calcein-AM (1 mg/mL for 15 min), and then observed by confocal laser scanning biological microscope (Olympus FluoView FV1000).

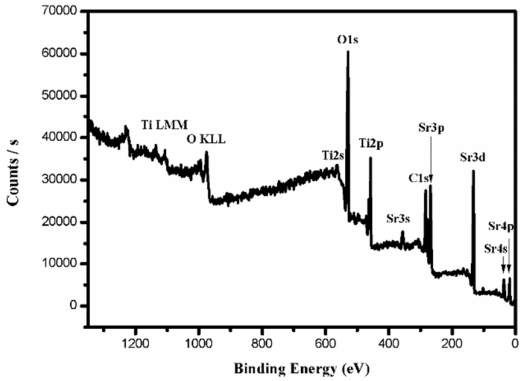

Figure 2. The XPS survey of the $SrTiO_3$ nanocrystals.

Figure 3. (a) SEM image of single typical $SrTiO_3$ nanocrystal, (b) TEM image of one typical $SrTiO_3$ nanocrystal, (c) HRTEM image on the edge, and (d) the corresponding SEAD pattern viewed along <001>.

The XRD pattern (Fig.1) of the nanocrystals shows that all the diffraction peaks agree perfectly with those of $SrTiO_3$ perovskite phase (JCPDS No. 35-0734) and without any impurity phase. These indicate the resulting nanocrystals is well-developed and pure $SrTiO_3$ with perovskite phase. The surface chemical composition is clearly demonstrated in the XPS (Fig.2). The surface of the cubic nanocrystals is composed of O, Ti, Sr, which is consistent with compound $SrTiO_3$. There is no other element on the surface. Atomic ratio of Ti and Sr on the surface of the nanocrystal is 1.1:1, which means that Ti is

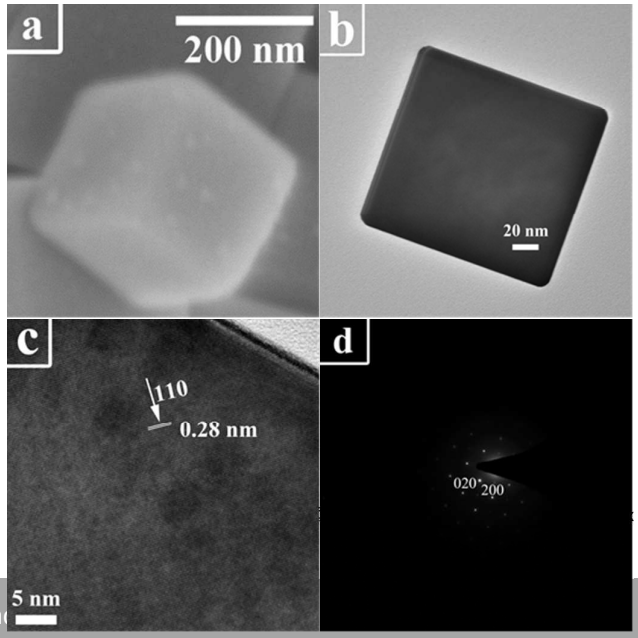

more than Sr comparison with the bulk interior, and a little Sr deficiency on surface appears. The excrescent C and O are from the surrounding atmosphere.

As shown in Fig.3a, the SEM image of one typical $SrTiO_3$ nanocrystal shows that the morphology of the nanocrystal is cubic. In Fig.3b, $SrTiO_3$ nanocrystals show to grow in a square shape with sharp 90-degree corners, and the side length of 200nm. The high-resolution transmission electron microscope (HR-TEM) image (Fig.3c) shows that the cubic nanocrystal has an interplanar spacing of 0.28 nm, which means the family of crystal planes attributed to (110). And the selected-area electron diffraction (SAED) patterns (Fig.3d) from a cubic nanocrystal proves that $SrTiO_3$ is single-crystalline and the cubic nanocrystal has well-developed {100} facets.

To engineer the nano-microstructured topography, spinning of $SrTiO_3$ nanocrystals experiments were carried out. By controlling the spinning speeds, the morphology of the resulting surfaces results in significantly different stacking density of $SrTiO_3$ cubic nanocrystals. As can be seen in Fig.4, the lower speed leads to a higher density. The number of the nanocrystals on the substrate was calculated on different area in average. Hence the number in the low-density (Fig.4a) is about 2.33×10^6 per mm^2 in average. And the number of the high-density (Fig.4b) is about 5.83×10^6 per mm^2 in average.

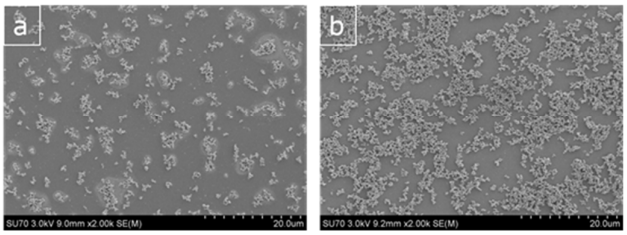

Figure 4. SEM images of the nano-microstructured surfaces obtained at different spinning speed (a) 8000 r/min, (b) 2000 r/min.

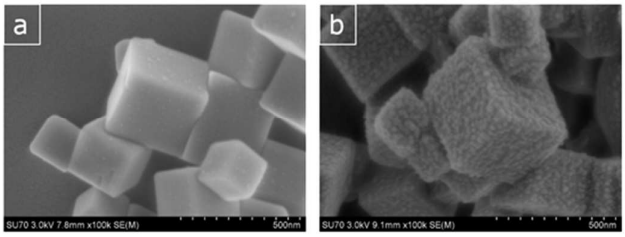

Figure 5. SEM images of the nano-microstructured surface, (a) without and (b) with BSA adsorption for 24 hours.

BSA was used as the model protein to evaluate protein adsorption capacity of the nano-microstructured surfaces. After immersing into BSA solution for 24 hours, the surface of $SrTiO_3$ cubic nanocrystals is uniformly and thickly covered with BSA proteins (Fig.5b), this also demonstrates that the exposed {100} facets of $SrTiO_3$ cubic nanocrystals have high affinity of protein adsorption.

The quantity of protein adsorbed on different nano-microstructured surfaces is showed in Fig.6. Compared with (100)-terminated $SrTiO_3$ single crystal substrate, the nano-microstructured surfaces with low or highly stacking density has higher BSA adsorption quantity. The BSA adsorption quantity of the surface with low stacking density is 10.64 μg/cm^2, and the highly stacking density is 15.97 μg/cm^2 and the single crystal substrate is 8.166 μg/cm^2. Moreover, the BSA adsorption quantity of the surface with highly stacking density is 50.1% more than that with low stacking density, and even 95.6% more than that of (100)-terminated $SrTiO_3$ single crystal substrate. The high BSA adsorption amount for the nano-microstructured surface with high stacking density is attributed to more {100} facets exposed on the surface.

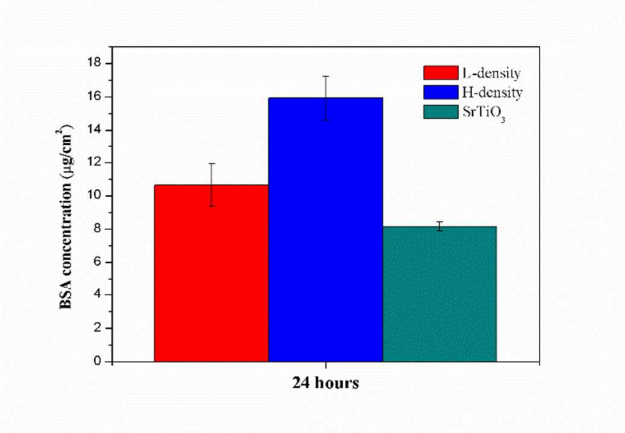

Figure 6. BSA adsorption quantity on low-density and high-density $SrTiO_3$ nanocrystal nano-microstructured surfaces and the (100)-terminated $SrTiO_3$ single crystal substrate was used as the control.

Figure 7. CCK-8 results of MC3T3-E1 cells cultured on different surfaces for 1 day and 3 days.

MC3T3-E1 cells cultured for 1 day was used to evaluate the ability for the cells to adhere on the surfaces. The nano-microstructured surfaces with both high and low stacking density have better cellular adhesion than the (100)-terminated $SrTiO_3$ single crystal substrate (Fig.7). The nano-microstructured surface with high stacking density is 55% in OD value more than the single crystal substrate. MC3T3-E1 cells cultured for 3 days was used to observe the cellular proliferation on the surfaces. Compared with the cells cultured for 1 day, the number of the cells on the surfaces all increases,

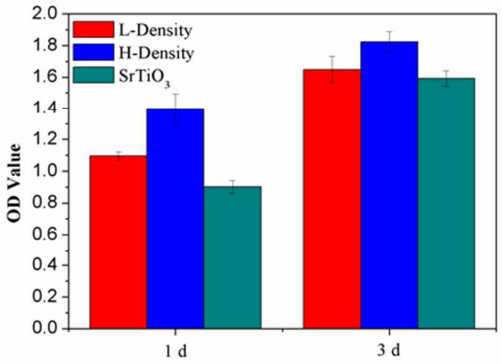

and the difference among the three surfaces has a similarity to the adhesion.

Calcein-AM assay was adopted to evaluate cellular morphology. For 1 day cultured cells, the cells cultured on the nano-microstructured surfaces (Fig.8a and b) shows stronger adhesion and spread morphology with long and multi-pseudopodia, comparing with that of (100)-terminated $SrTiO_3$ single crystal substrate (Fig.8c) in which the cells show minimal adhesion and relatively round morphology with almost none pseudopodium. For 3 days cultured cells, the cellular morphology on the three surfaces (Fig.8 d, e f) is kept like that of the 1 day cultured cells, and the situation in cell numbers is consistent with the CCK-8 results in Fig.7.

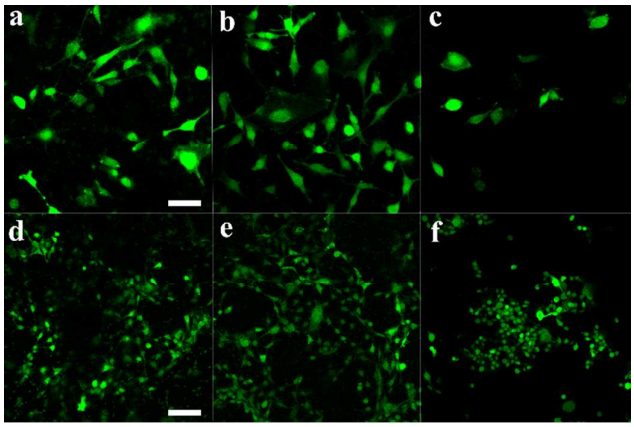

Figure 8. Fluorescence microscope images of Calcein-AM staining MC3T3-E1 cells cultured on (a) low stacking density, (b) high stacking density and (c) single crystal substrate for 1 day, and (d) (e) (f) for 3 days. Scale bar = 50 μm in a, b, c and scale bar = 100 μm in d, e, f.

For the enhancement in cellular responses in this work, two factors, total area for exposed {100} facets and surface topology, are suggested to play a crucial role. A little Sr deficiency in the surface composition of $SrTiO_3$ nanocrystals may give a higher specific protein affinity, and more {100} facets exposed on the surface can provide more interaction points. Therefore, the surface with high staking density of the nanocrystals can support stronger cellular responses as others reported.[25] In view of nano-microstructure, the cubic nanocrytals with 200nm side length can give ~200nm roughness between nanocrystals and ~1000nm roughness between nanoscrystal cluster and the substrate, both roughness in nano and micro scale are considered as ideal for cell growth.[26, 27] The better cellular responses of the {100} faceted cubic nanocrystals based surface than that of the smooth (100)-terminated $SrTiO_3$ single crystal surface further illustrate that a surface with topological structure facilitates cellular growth.

Conclusions

The nano-microstructured surfaces assembled by $SrTiO_3$ cubic nanocrystals with exposed {100} facets enhance the protein adsorption and subsequently cellular adhesion and proliferation. Moreover, the cellular response can be further enhanced by increasing the quantity of the protein adsorption. Our work indicates that a nanocrystal with strong protein afinity will be a powerful structured unit for assembling nano-microstuctutres and can provide significant opportunities in terms of engineering the material-cell interactions.

Acknowledgements

This work is financially supported by the Postdoctoral Science Foundation of China (Grant No. 2015M570504), National Natural Science Foundation of China (51372217, 51272228), National Basic Research Program of China (973 Program, 2012CB933600), Zhejiang Province Key Science and Technology Innovation Team (Grant No. 2013TD02), and the Fundamental Research Funds for the Central Universities (2013QNA4010).

Notes and references

1. C. J. Wilson, R. E. Clegg, D. I. Leavesley and M. J. Pearcy, *Tissue engineering*, 2005, **11**, 1-18.
2. H. Chen, L. Yuan, W. Song, Z. Wu and D. Li, *Progress in Polymer Science*, 2008, **33**, 1059-1087.
3. M. A. Schwartz and M. H. Ginsberg, *Nat Cell Biol*, 2002, **4**, E65-68.
4. M. S. Lord, M. Foss and F. Besenbacher, *Nano Today*, 2010, **5**, 66-78.
5. R. J. Miron, D. D. Bosshardt, E. Hedbom, Y. Zhang, B. Haenni, D. Buser and A. Sculean, *J Periodontol*, 2012, **83**, 936-947.
6. V. Hlady, J. Buijs and H. P. Jennissen, *Methods Enzymol*, 1999, **309**, 402-429.
7. A. E. Nel, L. Mädler, D. Velegol, T. Xia, E. M. Hoek, P. Somasundaran, F. Klaessig, V. Castranova and M. Thompson, *Nature materials*, 2009, **8**, 543-557.
8. M. Malmsten, *Colloids and Surfaces B: Biointerfaces*, 1995, **3**, 297-308.
9. C. F. Wertz and M. M. Santore, *Langmuir*, 2001, **17**, 3006-3016.
10. A. Gessner, A. Lieske, B. Paulke and R. Muller, *Eur J Pharm Biopharm*, 2002, **54**, 165-170.
11. N. Podhipleux, V. Krisdhasima and J. McGuire, *Food Hydrocolloid*, 1996, **10**, 285-293.
12. J. H. Forstater, A. Kleinhammes and Y. Wu, *Langmuir*, 2013, **29**, 15013-15021.
13. J. E. Gagner, X. Qian, M. M. Lopez, J. S. Dordick and R. W. Siegel, *Biomaterials*, 2012, **33**, 8503-8516.
14. L. Dong, Q. Luo, K. Cheng, H. Shi, Q. Wang, W. Weng and W. Q. Han, *Scientific reports*, 2014, **4**, 5084.
15. J. Fiedler, B. Ozdemir, J. Bartholoma, A. Plettl, R. E. Brenner and P. Ziemann, *Biomaterials*, 2013, **34**, 8851-8859.
16. C. J. Oates, W. Y. Wen and D. W. Hamilton, *Materials*, 2011, **4**, 893-907.
17. T. M. Lee, R. S. Tsai, E. Chang, C. Y. Yang and M. R. Yang, *J Mater Sci Mater Med*, 2002, **13**, 341-350.
18. R. Lange, F. Luthen, U. Beck, J. Rychly, A. Baumann and B. Nebe, *Biomol Eng*, 2002, **19**, 255-261.

19. L. E. Carneiro-Campos, C. P. Fernandes, A. Balduino, M. E. Leite Duarte and M. Leitao, *Clin Oral Implants Res*, 2010, **21**, 250-254.
20. D. H. Kim, C. H. Seo, K. Han, K. W. Kwon, A. Levchenko and K. Y. Suh, *Adv Funct Mater*, 2009, **19**, 1579-1586.
21. S. B. Kennedy, N. R. Washburn, C. G. Simon, Jr. and E. J. Amis, *Biomaterials*, 2006, **27**, 3817-3824.
22. J. Wei, T. Igarashi, N. Okumori, T. Igarashi, T. Maetani, B. Liu and M. Yoshinari, *Biomed Mater*, 2009, **4**, 045002.
23. B. G. Keselowsky, D. M. Collard and A. J. Garcia, *Journal of biomedical materials research. Part A*, 2003, **66**, 247-259.
24. C. R. Jenney and J. M. Anderson, *J Biomed Mater Res*, 2000, **49**, 435-447.
25. R. Agarwal and A. J. Garcia, *Adv Drug Deliv Rev*, 2015, DOI: 10.1016/j.addr.2015.03.013.
26. K. J. Cha, J. M. Hong, D. W. Cho and D. S. Kim, *Biofabrication*, 2013, **5**, 025007.
27. A. Wennerberg and T. Albrektsson, *Int J Oral Maxillofac Implants*, 2000, **15**, 331-344.